pagepress

Journal of Limnology
CNR - Water Research Institute (IRSA) - Verbania Pallanza - Italy

JOURNAL OF LIMNOLOGY

DOI: 10.4081/jlimnol.2024.2173

SUPPLEMENTARY MATERIAL

Polarised light pollution on river water surfaces caused by artificial light at night from illuminated bridges and surroundings

Catherine Pérez Vega,[1,2*] Franz Hölker,[1,2] Karolina M. Zielinska-Dabkowska,[3] Andreas Jechow[1,4]

[1]Leibniz Institute of Freshwater Ecology and Inland Fisheries (IGB), Berlin, Germany
[2]Department of Biology, Chemistry, and Pharmacy, Institute of Biology, Freie Universität Berlin, Germany
[3]GUT Light Lab, Faculty of Architecture, Gdansk University of Technology, Gdansk, Poland
[4]Department of Engineering, Brandenburg University of Applied Sciences, Brandenburg an der Havel, Germany

***Corresponding author:** catherine.perez@igb-berlin.de

Electromagnetic radiation is a transverse wave where the electromagnetic field oscillates perpendicular to the wave's propagation direction. Thus, this oscillation can be directional as well, which is called polarisation. Light is unpolarised when the electric field has equal amplitude in all directions, the direction of the electric field oscillates equally in all spatial directions and randomly in time (i.e., with random phase), as shown in Fig. S1a (left). If the oscillation of the electric field aligns along a single plane, then it is defined as linearly polarised, as shown in Fig. S1a (right), as an example, after passing through a linear polariser, resulting in linear polarisation in the y-axis. Unpolarised light can become polarised when it is reflected or transmitted at surfaces that have a preference for reflecting or transmitting polarised light due to their material properties (Foster *et al.*, 2018). When the electric field oscillates perpendicular to the incidence plane (which is confusingly not the material surface plane itself but the normal plane in the incidence direction of the light beam), this is called s-polarisation. When the electric field oscillates parallel with respect to the incidence plane, then it is known as p-polarisation. This is illustrated in Fig. S1 b,c.

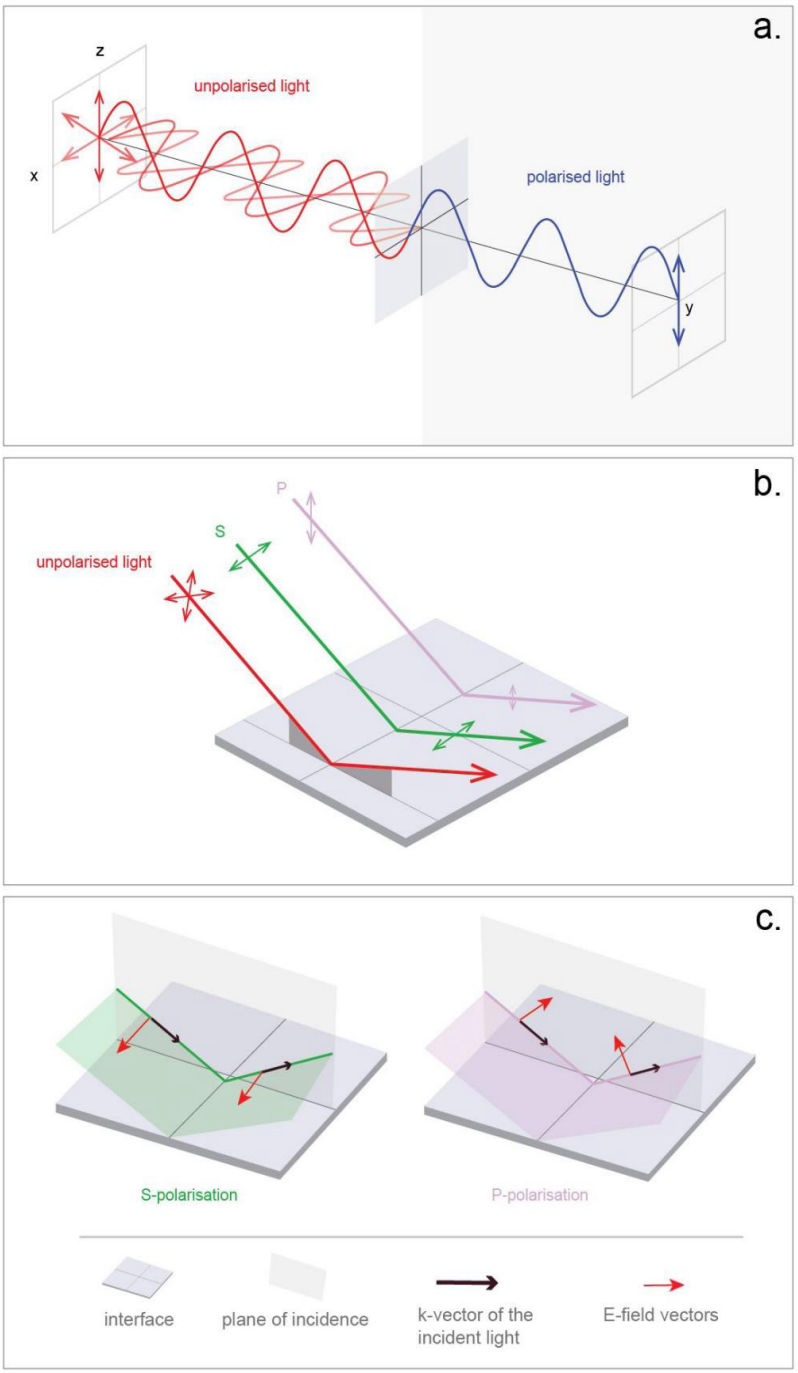

Fig. S1. a) Unpolarised (red, on the left) and linearly polarised light reflected after passing through a polariser (blue, to the right). b,c) Comparison of reflected s- (green) and p- (purple) polarised beams at the surface. S-polarisation (in green) polarises its beam parallel to the surface and has the electric field oscillating perpendicular to the water (S for senkrecht/perpendicular to the incidence plane). P-polarisation (in purple) polarises its beam perpendicular to the surface and has the electric field oscillating perpendicular to the water surface (P for parallel/parallel to the incidence plane). Source: author's own work and modified from Foster *et al*. 2018.

When an incident ray of light travels through air and reaches the water, light can change by reflectance, transmission, or both at the boundary of these two materials, as shown in Fig. S2, with incident (θ_I) reflected (θ_R), and refracted (θr) angles to the normal line (the dashed line) perpendicular (90° angle) to the surface at the point of incidence, as shown in Fig. S1. Incident and reflected angles are equal:

$$\theta_I = \theta_R \qquad \text{(eq. S1)}$$

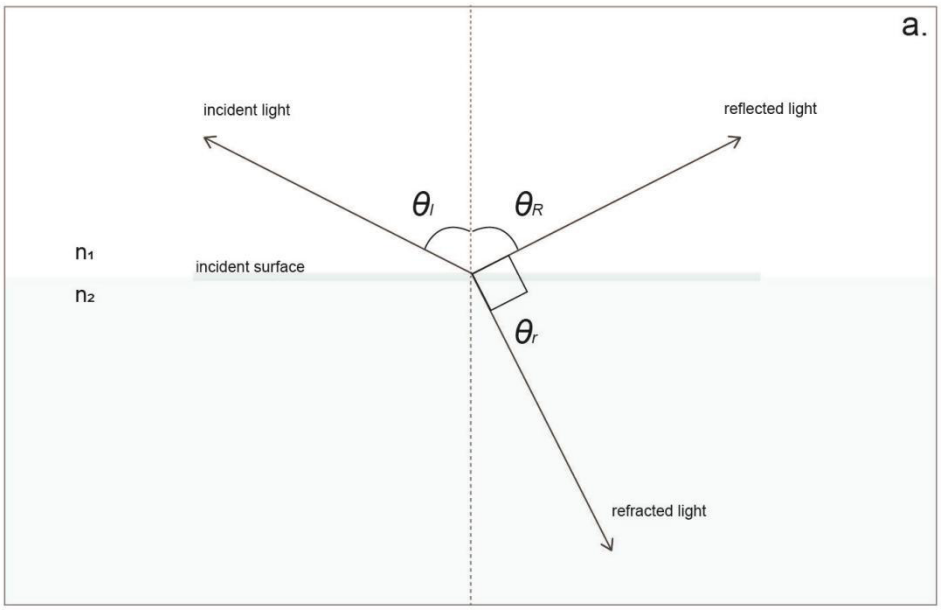

Fig. S2. Overview of incident light being polarised when travelling from air and striking at the water, in which n_1 is air and indicates the index of refraction of the incident medium, n_2 is water and indicates the index of refraction of the striking medium, and the angle of incidence from the normal (dashed line). The angle of refraction at this boundary is governed by the refractive indices of the involved materials. The index of refraction (n) is a property that indicates the ratio of the speed of light in a vacuum to the speed of light in the interested medium.

Snell's law determines the angle of refraction.

$$n_1 \, sin \, \theta_I \; = \; n_2 \, sin \, \theta_r \qquad \text{(eq. S2)},$$

Here, the first material is air ($n_1 \approx 1$) and the second material is water ($n_2 \approx 1.33$). This results in what is called Snell's window, with light incident almost horizontally ($\theta_I = 90°$) being refracted to an angle of 48.7°, which means that the full hemisphere with a 180° opening angle above the water is collapsed into a cone with an opening angle of only 97.4° underwater (see e.g. Fig. 3 a,b in Hölker *et al.*, 2023). Depending on the angle of incidence and the linear polarisation direction of the light (s- or p-polarisation), the reflection coefficient R will differ following the Fresnel equations (eq. 3 and 4), with the resulting coefficients shown in Fig. S3.

$$R_\mathrm{s} = \left| \frac{n_1 \cos\theta_\mathrm{i} - n_2 \cos\theta_\mathrm{t}}{n_1 \cos\theta_\mathrm{i} + n_2 \cos\theta_\mathrm{t}} \right|^2 = \left| \frac{n_1 \cos\theta_\mathrm{i} - n_2 \sqrt{1 - \left(\frac{n_1}{n_2} \sin\theta_\mathrm{i}\right)^2}}{n_1 \cos\theta_\mathrm{i} + n_2 \sqrt{1 - \left(\frac{n_1}{n_2} \sin\theta_\mathrm{i}\right)^2}} \right|^2, \qquad \text{(eq. S3)}$$

$$R_\mathrm{p} = \left| \frac{n_1 \cos\theta_\mathrm{t} - n_2 \cos\theta_\mathrm{i}}{n_1 \cos\theta_\mathrm{t} + n_2 \cos\theta_\mathrm{i}} \right|^2 = \left| \frac{n_1 \sqrt{1 - \left(\frac{n_1}{n_2} \sin\theta_\mathrm{i}\right)^2} - n_2 \cos\theta_\mathrm{i}}{n_1 \sqrt{1 - \left(\frac{n_1}{n_2} \sin\theta_\mathrm{i}\right)^2} + n_2 \cos\theta_\mathrm{i}} \right|^2. \qquad \text{(eq. S4)}$$

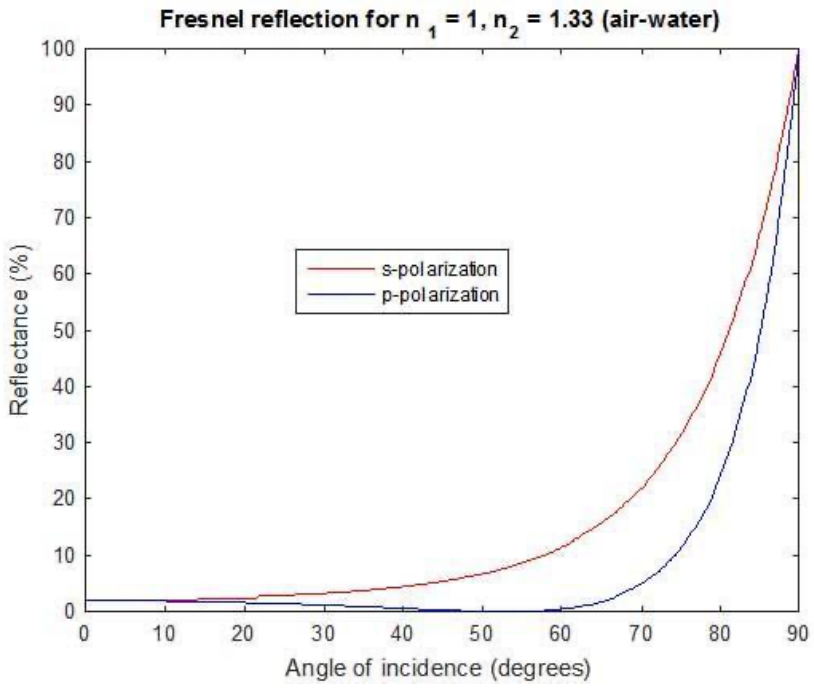

Fig. S3. Plot of the reflection coefficients as a function of angle of incidence, where total polarisation of reflected light (s-polarisation) occurs at approximately 53°.

If unpolarised light is incident at the water surface, the reflected light is partially polarised for most incident angles. For example, for light incident from the normal (i.e., 90° from the water surface), both polarisations are reflected equally, resulting again in unpolarised light. Maximum polarisation is reached for Brewster's angle (θ_B)

$$tan\ \theta_B = \frac{n_2}{n_1} \qquad \text{(eq. S5)}$$

$$\theta_B = 53.06° \qquad \text{(eq. S6)}$$

Tab. S1. Position at which measurements were taken at each site.

Measurement site	Bridges	Latitude, Longitude	Time
A	Moltkebrücke	52° 31' 17.44" N, 13° 22' 6.18" E	19:21 -19:35
B	Kronprinzenbrücke	52° 31' 21.37" N, 13° 22' 27.44" E	19:42 - 19:47
C	Monbijou	52° 31' 20.7" N 13° 23' 36.2" E	20:06 - 20:12
D	Friedrichsbrücke	52° 31' 16.3" N 13° 23' 57.7" E	20:15 - 20:20
E	Jannowitzbrücke	52° 30' 52.3" N, 13° 24' 59.9" E	20:34 - 20:39
F	Oberbaumbrücke	52° 30' 09.6" N, 13° 26' 36.1"E	20:56 - 21:17
G	Abteibrücke	52° 29' 12.0" N, 13° 28' 47.10" E	21:39 - 21:33

Tab. S2. Pixel count on the total amount of pixels on the water‘s surface of each measurement site and high and nearly high DOLP (ranging from 0.6 to 1.0, blue channel) at the water‘s surface of each measurement site.

Measurement site	**Bridges**	**Total pixel count on the water‘s surface**	**DOLP signal pixel count on the water‘s surface**
A	Moltkebrücke	15658	1955
B	Kronprinzenbrücke	40761	4566
C	Monbijou	38086	1297
D	Friedrichsbrücke	35831	4796
E	Jannowitzbrücke	19537	1811
F	Oberbaumbrücke	29294	2211
G	Abteibrücke	61327	4199

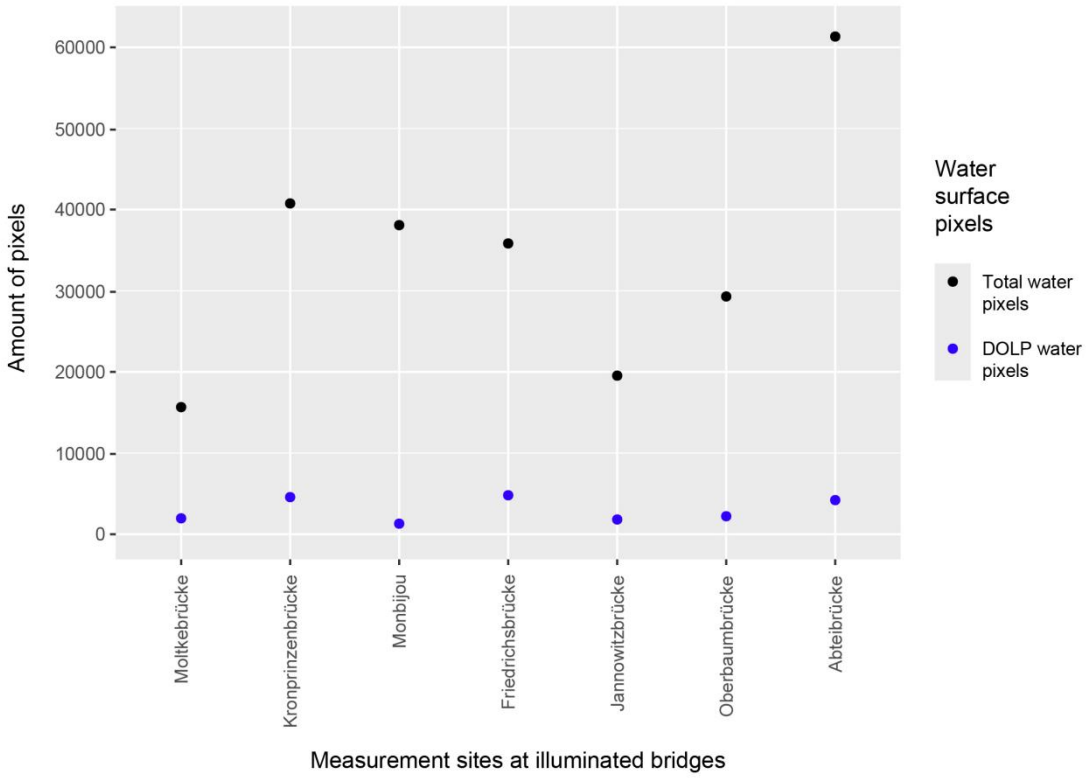

Fig. S4. Total water pixels (black dots) and high DOLP water pixels (blue dots) extracted from DOLP and RGB imaging data.

RGB images were created in R studio and rescaled in Image J to the exact size of its corresponding false colour plot. Both RGB and false colour images were transformed into 8-bit images. The water surface was identified manually from the RGB images and the water pixels counted by Image J. Then, a binary image was created form the DOLP data using a threshold of 60% and above (0.6 to 1.0). Non water pixels were removed from the analysis and Image J was used to count high DOLP water pixels. The percentage of high DOLP pixels to all water pixels was calculated.

References

Foster JJ, Temple SE, How MJ, Daly IM, Sharkey CR, Wilby D, Roberts NW, 2018. Polarisation vision: overcoming challenges of working with a property of light we barely see. Sci. Nat. 105:1-26.

Hölker F, Jechow A, Schroer S, Tockner K, Gessner MO, 2023. Light pollution of freshwater ecosystems: principles, ecological impacts and remedies. Phil Trans Roy Soc B. 378:20220360.